The June 9 Bolivia and March 9 Fiji deep earthquakes of 1994: I. Source processes

Paul Lundgren

Jet Propulsion Laboratory, California Inst. of Tech., Pasadena

Domenico Giardini

Dipartimento di Scienze Geologiche, III Università, Roma, Italy

Abstract, We examined the source characteristics of the 1994 deep earthquakes of Bolivia (June 9) and Fiji (March 9) over a period range of 1-1000 s using moment tensor and body wave analyses. Moment tensor inversions from 100-1000 s reveal that these two earthquakes were essentially point sources at very long period with insignificant isotropic and non-double couple components with scalar moments $M_o = 2.56 \times 10^{2}$ Nm for the Bolivia and $M_o = 0.26 \times 10^{2}$ Nm for the Fiji earthquakes. Body wave analysis for the Bolivia event reveals a 45 s duration, a nearly linear E-NE 1 km/s rupture on the subhorizontal focal mechanism plane giving a stress drop $\Delta\sigma = 114$ MPa. For the Fiji earthquake we find a change in focal mechanism and a linear 3 km/s rupture plunging shallowly to the north on the steep clipping nodal plane with a duration of at least 20 s and $\Delta\sigma = 14$ MPa. Both ruptures propagated parallel their null (σ_2) axis and suggests that their width is controlled by the thickness of the seismogenic volume in deep slabs.

Introduction

The March 9, 1994, Fiji (18.04° S, 178.41° W, $h = 563$ km) and the June 9, 1994, Bolivia (13.84° S, 67.55° W, $h = 631$ km; from the NEIS for both events) earthquakes were the. largest deep earthquakes in 24 years and recorded time, respectively. Physical models for the generation of deep earthquakes have been proposed which produce faultlike dislocations and seismic emissions [*Green and Burnley*, 1989; *Kirby et al.*, *1991*] required by seismic observations of double couple radiation patterns with an insignificant isotropic component [*Kawakatsu*, *1991*]. The volume. of the seismogenic core of the deep slab constrains physical models of deep slab material [*Kirby et al.*, 1991]. Planes of deep seismicity have been observed in most deep slabs, suggesting large thickness of the seismogenic portion in some deep subduction zones [*Giardini and Woodhouse*, *1984*; *Lundgren and Giardini*, *1992*].

We examine the sources of both earthquakes over a broad period range from 1-1000 s. Among the questions we seek to answer is what were the spatial geometries and stress drops of their sources and was there anomalous emission of seismic energy at very low frequency (1-10 mHz).

Moment Tensor Solutions

To obtain moment tensor solutions for the Fiji and Bolivia deep shocks, following *Giardini [1992] we* invert 6 hours of VLP waveforms recorded at 10 VBB stations (IRIS/GSN, Med. Net), selected to provide an evenly spaced global coverage of

low-noise records; a higher density of stations would not add further information in the frequency range used in our inversion [*Dufumier and Cara, 1995*]. Kernels are generated as complete synthetic seismograms by normal modes summation [*Woodhouse, 1988*], using PREM [*Dziewonski and Anderson, 1981*]. We invert for deviatoric moment tensor solutions and we investigate the deviation of the solution from a pure double couple mechanism. We also lift the constraint of a null moment tensor trace and invert for its isotropic component. However, since complete seismograms are dominated by shear wave energy, the resolution of the volumetric component is not optimal.

Figure 1 displays the moment tensor solutions for the two events, obtained inverting complex spectra in narrow (1 mHz) frequency bands between 1 and 8 mHz, and in the wide 1-8 mHz band (BB). All solutions have negligible non-double couple and isotropic components, in agreement with other studies [e.g. *Ekström, 1994; Kikuchi and Kanamori, 1994; Hara et al., 1995*], and wc show the best double couple from the full moment tensor.

The seismic moment for the Bolivia earthquake (2.56 × 102' Nm; $M_w = 8.2$) and its fault geometry, with a sub-horizontal plane ($\phi = 311°$, $\delta = 1\ 1$", $\lambda = -510$), arc. in excellent agreement with the CMT solutions obtained at Harvard (2.63 x 10^{21} Nrn) and by *Kikuchi and Kanamori [1994] (3.0* x 102' Nm). The seismic moment of the Fiji earthquake (0.26 x 1 0^{21} Nm; $M_w = 7.5$) and the fault geometry ($\phi = 6°$, $\delta = 78°$, $\lambda = -1\ 12°$) arc also in agreement with the Harvard CMT (0.31 x 10^{71} Nm) and with the NEIC solution (0.23 x 1021 Nm). Wc estimate the source half-duration to bc 20 seconds for the Bolivia event and 13 seconds for the Fiji event.

Body Wave Inversion

To examine the spatiotemporal distribution of moment release of these earthquakes wc use the method of *Kikuchi and Fukao [] 985]*. This is an iterative technique which uses Greens functions for a fixed focal mechanism with the relative amplitudes for each phase (initial *P, p,* or s) determined by the focal geometry convolved with attenuation operators (t" = 1 s and 4 s for P and S waves respectively) and a triangular source time function element for each station on the assumed gridded fault plane. At each iteration the grid location and time of each subevent is calculated from the maximum correlation of the Greens function with the observed seismograms and with the constraint that they lie within a rupture velocity equal to the shear wave velocity from the origin (~6-7 km/s). Wc use Greens functions composed of the P, pP, sP, and *PP*, phases with time separation calculated from the IASP91 travel time. tables.. Wc include in our Greens function wavelets the surface reflected phases *pP, sP,* and *PP* since in general subevents on steeply dipping fault plane.s can occur over a significant depth interval. However, for near horizontal faults the inclusion of the depth phases with their often large amplitudes and possible unmodeled time delays duc to near source heterogeneity might be expected to degrade the solution. In the case of [hc Fiji earthquake, especially for near nodal stations in North America, [he *PP* phase arrives very near *sP* and at very large amplitude. For both earthquakes wc compared the solutions using just the *P* arrivals versus solutions using both the direct *P* and the depth phases and found little difference in the fit [o the main *P*

waveforms but greater scatter of subevents over the fault plane when we used only the direct P arrivals.

Bolivia Earthquake The stations used for the Bolivia event are shown in Figure 2(a). We usc 23, 360 s long P-wave displacement seismograms decimated to 0.7 s from the IRIS network. The first step was to try and determine the fault plane using the preliminary Caltech focal mechanism ($\phi = 90°$, $\delta = 82°$, $\lambda = -930$). We first inverted the seismograms for the. steeply dipping nodal plane with a range of depths from approximately 600-660 km. This gave a horizontal distribution of subevents at 640 km suggesting rupture on the subhorizontal plane. We then solved for the subhorizontal nodal plane centered at a depth of 640 km. The shallowly dipping plane. always gave a better fit (5% better) to the data and ruled out the steeply dipping plane.

Once we determined the shallow plane was the fault plane it was important to refine the focal mechanism. To do so we used the body wave moment tensor solution method of *Kikuchi and Kanamori [1991]*. We solv cd for the best mech anism using a 36 second triangular source time function at a depth of 640 km, and found $\phi = 346°$, $\delta = 14°$, $\lambda = -8°$.

To resolve the initial 10 seconds of the rupture and determine its location relative to the main area of moment release, we first solved for the main rupture using 8 s triangular time function elements and then solved for the initial 10 seconds of the rupture in three distinct time windows, each with a fixed focal mechanism and a time function element of 2 s duration (Fig. 3). Changes in the focal geometry from the main shock focal geometry for each time window were based on observed changes in the polarities at the three near nodal stations RAR, BOSA, and SUR.

Figure 3 shows the source time function, distribution of subevents on the shallowly dipping plane, and the tit of synthetic waveforms to the displacement seismograms. The fault plane grid is centered at a depth of 640 km. The seismic moment calculated was $MO = 2.5 \times 1$ 0^{21} Nm. To estimate the rupture areas wc take the rough areas over which the subevents arc spread, recognizing that we use point source Greens functions in our inversion and ignoring obvious non-causal outliers such as subevent number 1. The moment release areas of the initial (20x20 km 2, and main (50x20 km^2) rupture sequences allow us to calculate the average stress drop $= \Delta\sigma = 2.4 \times M_o S - {}^{1.5} = 114$ MPa. This value is very high compared to shallow car thquakes but not unusual for earthquakes at this depth [*Chung and Kanamori*, 1980]. The small area and short duration gives a slow 1 km/s rupture velocity. These results are very much in agreement with those reported by *Kikuchi and Kanamori [1994]*. The slight differences in rupture probably result from the greater number and greater azimuthal distribution of stations wc used in our inversions. Inclusion of stations SUR, BOSA, and PM SA enhance the spatial resolution of the. source..

Fiji Earthquake For the Fiji event we followed the body wave inversion procedure described for the Bolivia event. We used P-wave seismograms with 1 s sampling rate from the 16 stations shown in Figure 2(b). The focal mechanism was chosen base.d on the P-wave polarities of the first arrivals and apparent change in focal mechanism dictated by the change, in polarity of the l'-wave displacement seismograms for stations in

North America (excluding Alaska stations) and Hawaii. The geometry of the NW dipping nodal plane was modified to better fit the near nodal stations in North America and Hawaii which have $P, pP, PP,$ and sP amplitudes which arc very sensitive to the focal mechanism. The focal mechanism for the second part of the rupture was modified from the initial mechanism to satisfy the polarities and amplitude ratios of the North America and Hawaii stations. The focal mechanisms were ($\phi = 16°$, $\delta = 66°$, $\lambda = -120°$) and ($\phi = 351°$, $\delta = 70$", $\lambda = -123°$) for the first and second portions of the rupture respectively.

Figure 4 shows our preferred solution for this earthquake. We used [ime function elements of 3 s duration. The rupture occurred on the steeper, northerl y striking pl ane centered at a depth of 575 km which always gave a better fit to the displacement seismograms, consistent with the findings of Wiens et al. [1994]. The solution shown in Figure 4 forms a very simple linear rupture towards the north, roughly parallel the null axis of the focal mechanism which plunges shallowly towards the north. The seismic moment calculated from the body waves was $M_o = 1.9 \times 10^{20}$ Nm with rupture duration of 17 s. The spatial extent of the rupture was 60 x 20 km^2 giving a $\Delta\sigma = 14$ MPa, much lower than the Bolivia earthquake stress drop but within the normal range for deep earthquakes [Chung and Kanamori, 1980]. The rupture velocity for this event was 3 km/s which is slow compared to the shear velocity, though much faster than for the Bolivia event.

Discussion and Conclusions

The occurrence of these two great deep earthquakes several months apart and with the availability of broad band digital seismograms allows a unique opportunity to compare in some detail their source characteristics. The moment tensor analysis shows no anomalous characteristics below 1 mHz and no significant isotropic component, Neither arc the geometries of the rupture plants particularly unexpected (see Giardini and Lundgren this issue) since both earthquakes feature focal mechanisms compatible with down-dip compression appropriate for their local subduction zone geometries. While analysis of large deep focus earthquakes has found a propensity for rupture on steep planes [Fukao and Kikuchi, 1987], shear planes have been observed in many areas of deep seismicity which parallel shallow, steep, or both focal planes [Giardini and Woodhouse, 1984; Lundgren and Giardini, 1992].

The main interest in these earthquakes lies in the detai Is of their ruptures. The Bolivia earthquake ruptured over a surprisingly small area with a high stress drop. The Fiji earthquake, though an order of magnitude smaller, ruptured over a similar area with a much lower stress drop. The stress drops wc calculate for both earthquakes arc well within what has been calculated by Chung and Kanamori [1980] for deep earthquakes in Tonga and tits the pattern they found of lower stress drops in areas of higher seismicity and high stress drops in areas of lower seismicity. The difference these earthquakes exhibit in size given their similar rupture areas may reflect the differences in deep seismicity found in the Tonga and South America subduction zones [Giardini, 1988]. The greater amount of background seismicity and the greater number of aftershocks [Wiens et III., 1994] for the Fiji earthquake compared to the Bolivia earthquake support these observations. Both c.vents have nearly

linearly propagating ruptures parallel the focal mechanism intermediate axis (σ_2) direction and perpendicular to the slip direction. This propagation may be similar to that observed for large shallow subduction zone earthquakes [*Ruff and Kanamori, 1983]: the* earthquake ruptures the available width and length of the fault surface capable of moment release. For shallow underthrusting earthquakes seismic slip is possible only in the upper 40 km of the plate interface but the length may be hundreds of kilometers. For large deep earthquakes this analogy would suggest that the width of the zone capable of seismic moment release is on the order of 20-30 km. However, this remains quite speculative since our understanding of the detailed structure of deep subducted lithosphere and the physical mechanism for maintaining or terminating deep earthquake ruptures remains quite limited.

References

Chung, W.-Y., and H. Kanamori, Variation of seismic source parameters and stress drops within a descending slab and its implications in plate mechanics, *Phys. Earth Planet. Inter.*, 23, 134-159, 1980.

Dufumier, 11. and M. Cara, On the limits of linear moment tensor inversion of surface wave spectra, *Pure App. Geophys.*, in press, 1995.

Dziewonski, A.M. and D. 1. Anderson, Preliminary Reference Earth Model (PREM), *Phys. Earth Planet. Inter.*, 25, 297-356, 1981.

Ekström, G., Teleseismic analysis of the great 1994 Bolivia earthquake, *EOS, Trans. Am. Geophys. Un.*, 75, 465, 1994.

Fukao, Y., Source process of a large deep-focus earthquake and its tectonic implications - the western Brazil earthquake of 1963, *Phys. Earth Planet. Interiors*, 5, 61-76, 1972.

Fukao, Y. and K. Kikuchi, Source retrieval for mantle earthquakes by iterative deconvolution of long-period J'-waves, *Tectonophysics, 144, 249-269, 1987.*

Giardini, D., Frequency distribution and quantification of deep earthquakes, *J. Geophys. Res., 93, 2095-2105, 1988.*

Giardini, D., Moment tensor inversion from MedNet data: (1) large worldwide earthquakes of 1990, *Geophys. Res. Lett.*, 19, 713-716, 1992.

Giardini, D., and P. Lundgren, The June 9 Bolivia and March 9 Fiji deep earthquakes of 1994: II. Geodynamic implication, *Geophys. Res. Lett., this issue,* 1995.

Giardini, D., and J. 11. Woodhouse, Deep seismicity and modes of deformation in Tonga subduction z.one, *Nature, 307, 505-509, 1984.*

Green, H. W., and P. C. Burnley, A new self-organizing mechanism for deep-focus earthquakes, *Nature, 341, 733-737, 1989.*

Hara, 'T., K. Kuge, and H. Kawakatsu, Determination of the isotropic component of the. 1994 Bolivia deep earthquake, *Geophys. Res. Lett., this issue,* 1995.

Kawakatsu, 11., Insignificant isotropic component in the moment tensor of deep earthquakes, *Nature, 351, 50-53, 1991.*

Kikuchi, M., and Y, Fukao, Iterative deconvolution of complex body waves from great earthquakes - the Tokachi-Oki earthquake of 1968, *Phys. Earth Planet. Inter., 37, 235-248, 1985.*

Kikuchi, M., and H. Kanamori, Inversion of complex body waves - 1[1, Bull. *Seismo. Sot. Amer.,* 81, 2335-2350, 1991.

Kikuchi, M. and H. Kanamori, The mechanism of the deep Bolivia earthquake of June 9, 1994, *Geophys. Res. Lett.,* 21, 2341-2344, 1994.

Kirby, S. H., W. B. Durham, and L. A. Stern, Mantle phase changes and deep-earthquake faulting in subducting lithosphere, *Science,* 252, 216-225, 1991.

Lundgren, P. R., and D. Giardini, Seismicity, shear failure and modes of deformation in deep subduction zones, *Phys. Earth Planet. Inter., 74, 63-74, 1992.*

Ruff, L., and H. Kanamori, The rupture process and asperity distribution of three great earthquakes from long-period diffracted P-waves, *Phys. Earth Planet. Inter., 31, 202-2.30, 1983.*

Wiens, D. A., J. J. McGuire, P. J. Shore, M. G, Bevis, K. Draunidalo, G. Prasad and S. P. Helu, A deep earthquake aftershock sequence and implications for the rupture mechanism of deep earthquakes, *Nature, .?72, 540-543, 1994,*

Woodhouse, J. H., The calculation of eigenfrequencies and eigenfunctions of the free oscillations of the Earth and the Sun, in *Seismological Algorithms,* ed. D. J. Doornbos, pp. 321-370, Academic Press, 1988.

D. Giardini, Dipartimento di Scienze Geologiche, III Università, via Ostiense 169, 00154 Roma, Italy (e-mail: giardini@in8800.ingrm.it)

P. Lundgren, JPL, 4800 Oak Grove Drive, Pasadena, CA 91109 (c-mail: paul@arrakis.jpl.nasa.gov)

Figure 1. Moment tensor solutions for the Bolivia and Fiji deep earthquakes obtained inverting complex spectra in narrow (1 mHz) frequency bands between 1 and 8 mHz, and in the wide 1-8 mHz band (BB). For each solution wc show the best double couple and we indicate the seismic moment, in units of 10^{2*} Nm.

Figure 2. Locations of stations used in the body wave inversions for the (a) Bolivia, and (b) Fiji earthquakes, center ed on their epicenters.

Figure 3. Bolivia earthquake body wave inversion results. (a) source time function, Short vertical lines separate time windows for inversions with different fixed focal mechanisms shown in (b). (b) focal mechanisms held fixed for diffc.rent time segments: for times 12-19 s and 21-53 s ($\phi = 346°$, $\delta = 14°$, $\lambda = -80$); for time windows 9-12 s and 19-21 s ($\phi = 270°$, $\delta = 25°$, $\lambda = -900$); (c) Gridded fault plane solution of subevents. The strike and dip of the plane arc indicated, with the bottom of the plane corresponding to increasing depth. Color and red number of subevents correspond in time to the red numbers and color bar shown with the source time function in (a). Subevents for the 10 s of initial rupture arc not numbered. (d) Data and synthetic (bold) seismograms for selected stations showing the P-wave displacement waveforms. Inversion results were computed from 360s of data for each station. (c) Data and synthetic (bold) seismograms for a few representative stations showing the entire waveforms used in drc

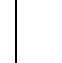inversion, inducting the later arriving depth phases.
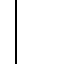
Figure 4. Fiji earthquake body wave inversion results. Explanation same as in Figure 3 with the exception for (b) where the focal mechanisms were ($\phi = 16°$, $\delta = 66°$, $\lambda = -120°$) and ($\phi 351°$, $\delta = 70°$, $\lambda = -123°$) for the first and second portions of the rupture, respectively; and in (c) where the clusters of subevents belonging to the two different fault plane geometries for the two focal mechanisms given in (b) for subevents shown in (a), arc roughly delineated by the dashed line,

LUNDGREN AND GIARDINI: THE 1994 BOLIVIA AND FIJI DEEP EARTHQUAKES

Fig 1

940609   Bolivia

2.24   2.36   262   2.66   2.52   2 36   2,64   256

940309   Fiji

0.21   0.24   0.26   0.26   0.25   0.25   0.24   0.26
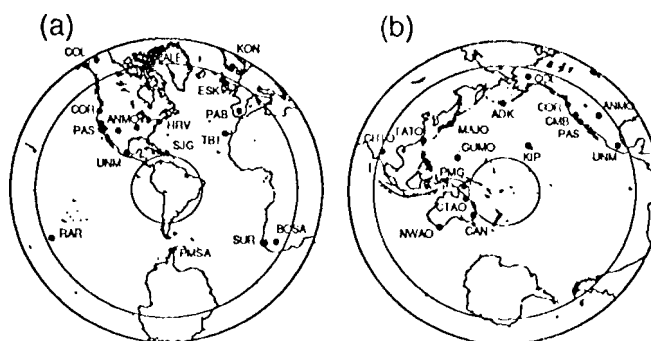
1-2   2-3   3-4   4-5   5-6   6-7   7-8   BB

(a)

(b)

Fig 2
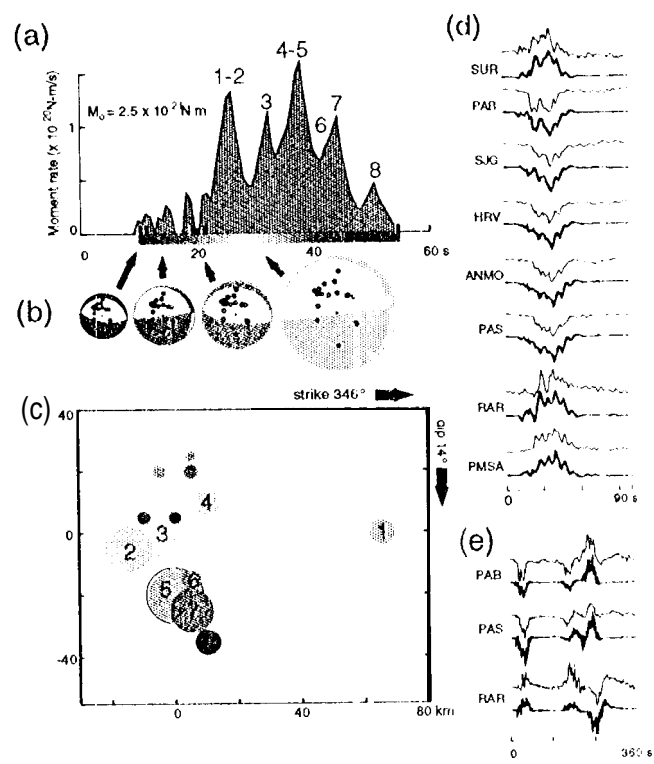Lundgren & Giardini
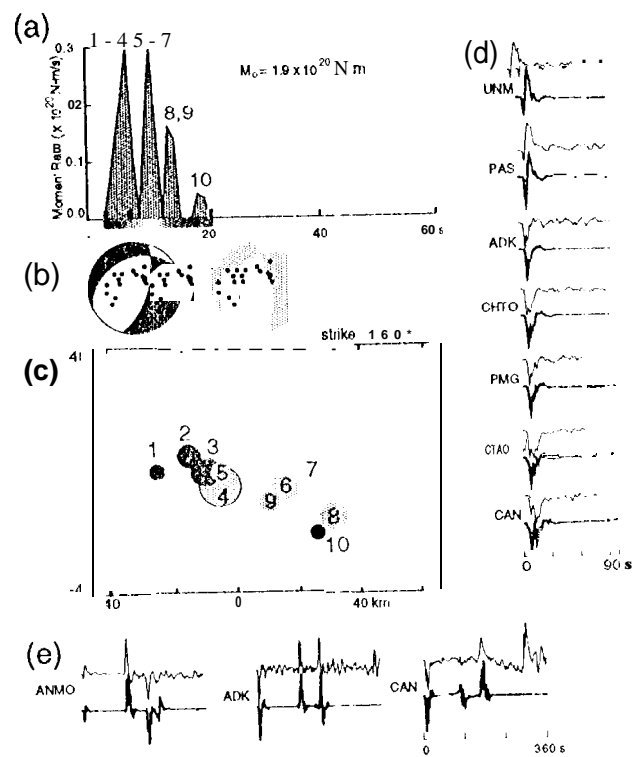
Figure 3

Figure 4